Blueshift of optical band gap in ZnO thin films grown by metal-organic chemical-vapor deposition

S. T. Tan, B. J. Chen, X. W. Sun,[a] and W. J. Fan
School of Electrical and Electronic Engineering, Nanyang Technological University, Nanyang Avenue, Singapore 639798, Singapore

H. S. Kwok
Department of Electrical and Electronic Engineering, The Hong Kong University of Science and Technology, Clear Water Bay, Kowloon, Hong Kong

X. H. Zhang and S. J. Chua
Institute of Materials Research and Engineering, 3 Research Link, Singapore 117602, Singapore

(Received 18 August 2004; accepted 29 April 2005; published online 1 July 2005)

The optical band gap of ZnO thin films deposited on fused quartz by metal-organic chemical-vapor deposition was studied. The optical band gap of as-grown ZnO blueshifted from 3.13 to 4.06 eV as the growth temperature decreased from 500 to 200 °C. After annealing, the optical band gap shifted back to the single-crystal value. All the ZnO thin films studied show strong band-edge photoluminescence. X-ray diffraction measurements showed that samples deposited at low temperatures (<450 °C) consisted of amorphous and crystalline phases. The redshift of the optical band gap back to the original position after annealing was strong evidence that the blueshift was due to an amorphous phase. The unshifted photoluminescence spectra indicated that the luminescence was due to the crystalline phase of ZnO, which was in the form of nanocrystals embedded in the amorphous phase. © *2005 American Institute of Physics*. [DOI: 10.1063/1.1940137]

I. INTRODUCTION

Zinc oxide (ZnO) is a wide direct band-gap (3.37 eV) semiconductor with a broad range of applications including light-emitting devices,[1] varistors,[2] solar cells,[3] and gas sensors.[4] Moreover, ZnO is a promising material for short-wavelength optoelectronic devices, especially for ultraviolet (UV) light-emitting diodes (LEDs) and laser diodes (LDs), due to its large exciton binding energy of 60 meV.[5,6] This exciton binding energy is much larger than the room-temperature thermal energy (26 meV), suggesting that the electron-hole pairs are stable even at room temperature. Therefore, efficient UV LEDs and LDs operating at room temperature can be expected, provided that high-quality *p*-type ZnO is available.[7,8]

In the past decade, ZnO thin films have been intensively studied and fabricated by various methods.[6,9–11] Metal-organic chemical-vapor deposition (MOCVD) is believed to be a promising method to achieve high-quality ZnO thin films.[11] As well, most reports focus on methods of obtaining single-crystal ZnO thin films, while there is little attention paid to amorphous and nanocrystalline ZnO. However, nanocrystal-embedded ZnO thin films possess some unique advantages over bulk crystalline ZnO thin films. According to Refs. 12 and 13, the refractive index of ZnO decreases gradually in the vicinity of the grain boundaries. Thus, such grain boundaries can behave as self-assembled laser cavities for random lasing in ZnO thin films. Therefore, it is worthwhile to study the crystal structure of ZnO thin films in the presence of a random amorphous phase. In this paper, the blueshift of the optical band gap of nanocrystal-embedded ZnO thin films grown at various temperatures is investigated.

II. EXPERIMENT

The ZnO thin films used in this study were grown on fused quartz (SiO_2) by MOCVD. The growth temperature ranged from 200 to 500 °C with an increment of 50 °C. Dimethylzinc (DMZn), N_2 gas, and high-purity O_2 were used as the zinc source, carrier gas, and oxidizing agent, respectively. The flows of DMZn and O_2 were set at 30 and 20 SCCM (standard cubic centimeter per minute). The DMZn bubbler was kept at −10 °C in a coolant bath. The chamber pressure was maintained at about 30 mbar and the deposition time for all the samples was 10 min. Postdeposition annealing, if any, was carried out in a mixed O_2 and N_2 ambient at 500 °C for 10 min.

The optical transmission spectra were measured with an UV-2501PC spectrophotometer at room temperature. The crystalline structure of the films was characterized by x-ray diffraction (XRD) measurement with Cu $K\alpha$ radiation (Siemens D5005 x-ray diffractometer). The photoluminescence (PL) spectra were measured with a micro-PL excited by the 325-nm line of a 30-mW He–Cd laser and detected with a charge-coupled device (CCD) array at room temperature.

III. RESULTS AND DISCUSSION

Figure 1 illustrates the transmission spectra for the ZnO films grown at various growth temperatures from 200 to 500 °C. The transmittances are over 80% in the vis-

[a]Author to whom correspondence should be addressed; electronic mail: exwsun@ntu.edu.sg

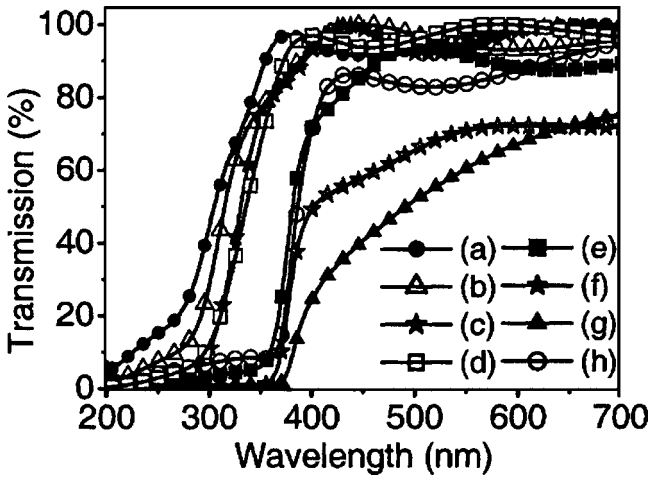

FIG. 1. Transmission spectra for the ZnO films grown at various temperatures: (a) 200 °C, (b) 250 °C, (c) 300 °C, (d) 350 °C, (e) 400 °C, (f) 450 °C, (g) 500 °C, and (h) grown at 350 °C and annealed at 500 °C for 10 min.

ible region for all the samples except for films grown at 450 °C, Fig. 1(f), and 500 °C, Fig. 1(g). The interference fringes indicate that all the ZnO films had optically smooth surfaces and that the interface with the quartz substrate is also smooth. It can be seen from Fig. 1 that an absorption tail near 280 nm is present for films grown below 400 °C. Also, the absorption edge shifted to shorter wavelength as the growth temperature decreases. This phenomenon can be observed clearly in Fig. 2, which shows the relationship between absorption coefficient as a function of photon energy.

The absorption coefficient α can be calculated from the relation:[11]

$$T = A \exp(-\alpha d), \tag{1}$$

where T is the transmittance of thin film, A is a constant, and d is the film thickness. The constant A is approximately

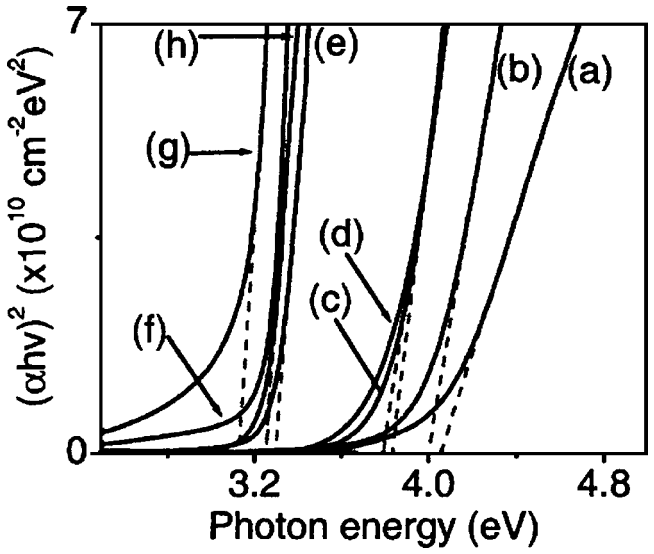

FIG. 2. Plot of $(\alpha h\nu)^2$ vs photon energy for ZnO films grown at various temperatures: (a) 200 °C, (b) 250 °C, (c) 300 °C, (d) 350 °C, (e) 400 °C, (f) 450 °C, (g) 500 °C, and (h) grown at 350 °C and annealed at 500 °C for 10 min.

TABLE I. Estimated optical band gap of ZnO films at various growth temperatures.

Sample	Growth temperature (°C)	Estimated optical band gap (eV)
a	200	4.06
b	250	4.00
c	300	3.84
d	350	3.79
e	400	3.30
f	450	3.25
g	500	3.13
h	350+annealing	3.25

unity, as the reflectivity is negligible and insignificant near the absorption edge. The optical band gap of the films is determined by applying the Tauc model,[14] and the Davis and Mott model[15] in the high absorbance region:

$$\alpha h\nu = D(h\nu - E_g)^n, \tag{2}$$

where $h\nu$ is the photon energy, E_g is the optical band gap, and D is a constant. For a direct transition, $n=1/2$ or $2/3$ and the former value was found to be more suitable for ZnO thin films since it gives the best linear curve in the band-edge region.[11,16] In Fig. 2, the relationship between $(\alpha h\nu)^2$ and $h\nu$ is plotted. The E_g value can be obtained by extrapolating the linear portion to the photon energy axis in that figure. The optical band-gap values obtained are summarized in Table I. As the growth temperature was reduced from 500 to 200 °C, the optical band gap blueshifted from 3.13 to 4.06 eV. A similar blueshift phenomenon of optical band gap was also observed in ZnO thin films deposited on sapphire substrate.[11]

We also noticed that if the sample was annealed, there would be a redshift of the band gap. Figure 2(d) shows the band gap for a sample grown at 350 °C while Fig. 2(h) shows the same sample after annealing. The absorption edge redshifts from 3.79 to 3.25 eV. The sample grown at 350 °C was chosen as an example for clarity. In fact, all the annealed samples showed an optical band gap of around 3.25 eV.

Figures 3(a) and 3(b) show the typical XRD profiles of the as-grown ZnO films at various growth temperatures from 200 to 500 °C with an increment of 50 °C. Figure 3(c) shows the XRD profiles of the as-grown and annealed samples. It was found that all as-grown films exhibit polycrystalline structure. Using the background noise level as a reference, it can be seen that the crystallinity of all the films grown at low temperatures from 200 to 400 °C is poor, as shown in Figs. 3(a) and 3(b).

The XRD measurements show that the ZnO thin films obtained contain nanocrystals. The grain sizes vary from 5 to 13 nm according to Scherrer's formula:

$$t = \frac{C\lambda}{B\cos\theta}, \tag{3}$$

where B is the full width at half maximum [(FWHM) in radians] of XRD yields, λ is the x-ray wavelength (Cu $K\alpha$ =0.154 nm), θ is the Bragg diffraction angle, and C is a correction factor which is taken as 1. The estimated grain size at crystallographic plane (002) was summarized in Table

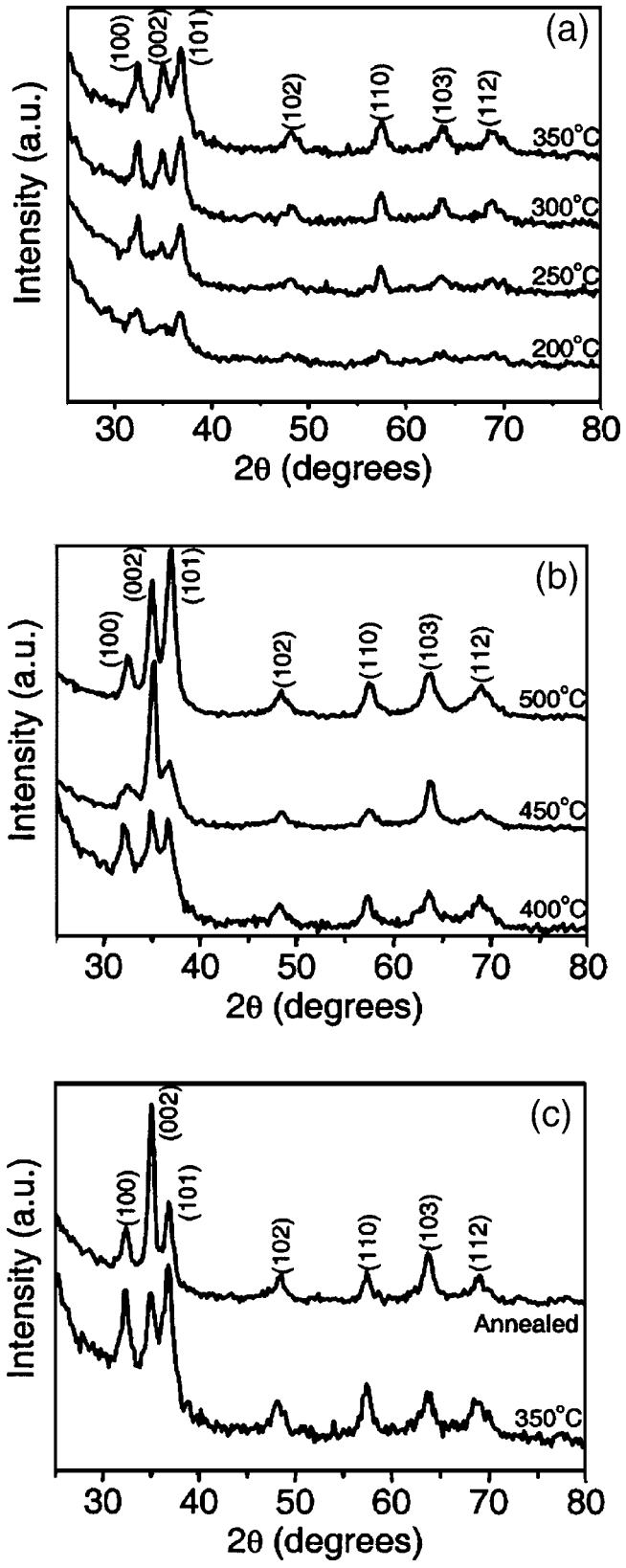

FIG. 3. XRD profiles of ZnO films grown at various temperatures: (a) 200–350 °C, (b) 400–500 °C, and (c) grown at 350 °C and annealed at 500 °C for 10 min.

II. From Table II, it can be seen that the estimated grain size ranges from 5 to 13 nm for crystallographic plane (002). It should be mentioned that the grain size should not be uniform and the estimated value may not be exact, which can be seen from Table II that the grain size does not increase monotonically with temperature.

TABLE II. Estimated grain size of crystallographic plane (002) of ZnO films at various growth temperatures.

Growth temperature (°C)	Grain size (nm) in crystallographic plane (002)
200	5.57
250	7.66
300	9.93
350	8.85
400	8.75
450	14.69
500	10.11
350+annealing	13.55

From the XRD results, we propose that the absorption edge blueshift is due to the poor crystallinity of ZnO thin films grown at low temperature. The crystallinity of the ZnO thin films grown below 400 °C was poor and exhibits polycrystalline structure. The physical model of the structure can be viewed as various nanocrystalline islands embedded in a matrix of amorphous ZnO. Qualitatively, the interatomic spacing of amorphous structure would be relatively long and more disordered than crystalline structure due to the absence of long-range translational periodicity. As the fraction of amorphous ZnO phase increases in the films grown at low temperature, the extended localization in the conduction and valence bands increases.[11] As a result, the absorption of photon is mainly contributed by amorphous ZnO and hence the absorption edge blueshifted. On the other hand, for samples grown at higher temperature (>400 °C), the crystallinity of ZnO thin films becomes better. The optical band gap reduces to that of the crystalline ZnO.

The poor crystal quality of the films grown at low temperature can be greatly improved by annealing. It can be seen from Fig. 3(c) that the *c*-axis orientation was improved significantly after the annealing process, with FWHM of (002) reduces from 1.04°to 0.68°. In order to distinguish the effect of crystallite-size-induced broadening and strain-induced broadening at FWHM of the XRD profile, the Williamson–Hall plot[17] was performed and shown in Fig. 4. The crystal-

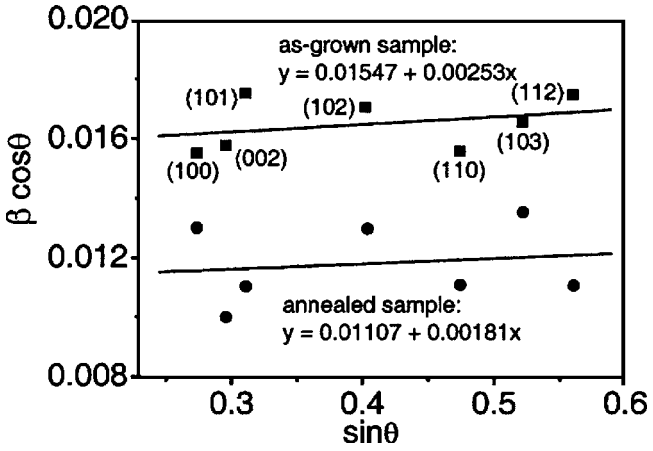

FIG. 4. Williamson–Hall plots for as-grown and annealed ZnO films.

line size and strain can be obtained from the intercept at the y axis and the slope, respectively:

$$B\cos\theta = \frac{C\lambda}{t} + 2\varepsilon\sin\theta, \tag{4}$$

where B is FWHM in radians, t is the grain size in nanometers,ε is the strain, λ is the x-ray wavelength in nanometers, and C is a correction factor which was taken as 1. The grain size and strain of the as-grown sample were found to be 9.95 nm and 1.265×10^{-3}, respectively. After annealing, the grain size increased to 13.9 nm while the strain reduced to 9.05×10^{-4}. Through the annealing process, the strained or partially strained ZnO structures will be relaxed. However, as is seen from the Williamson–Hall plot, the strain values are very small and thus their effect on broadening is negligible. As a result, the redshift of the optical band gap after annealing is due to the improved crystallinity of the film, which acts as a strong evidence that the blueshift phenomenon of optical band gap is due to the amorphous phase ZnO in the as-grown films.

The PL of the ZnO thin films was measured at room temperature. Wide band-edge emission spectra ranging from 3 to 3.6 eV were observed for all the samples while the green band emission was observed for films grown at temperature lower than 350 °C (not shown here). The wide range of emission spectrum should be due to the nanocrystalline phase, as the amorphous phase should not emit well. The emission by the nanocrystalline structure will have the similar quantum size effect as quantum dots and can be described by the following equation:[18,19]

$$E_{(\mathrm{gap,nanocrystal})} = E_{(\mathrm{gap,bulk})} + \frac{\pi^2\hbar^2}{2R^2}\left(\frac{1}{m_e^*} + \frac{1}{m_h^*}\right) - 0.248E_{\mathrm{Ry}}^*. \tag{5}$$

The bulk band gap $E_{(\mathrm{gap,bulk})}$ is taken as 3.2 eV (Ref. 20) and the bulk exciton binding energy E_{Ry}^* can be taken as 60 meV.[6] According to Beni and Rice[21] and Fan *et al.*,[22] the electron and hole effective masses are taken as $m_e^*=0.24m_0$ and $m_h^*=2.31m_0$, respectively. Additionally, h is Planck's constant and R is the radius of ZnO nanocrystals.

Figure 5 shows a plot of the nanocrystal band gap $E_{(\mathrm{gap,nanocrystal})}$ versus the nanocrystal radius R. The solid curve is the theoretical fit of Eq. (5), while the symbols (○) are the grain sizes estimated from XRD result (Table II) and their corresponding band gaps measured from PL. From Fig. 5, it can be seen that the nanocrystal band gap of all the samples measured from the PL fits the theoretical curve. It is noticed that the band gap does not show much variation with the crystallite size, which corresponds to various growth temperatures (Table II). This is mainly because the crystallite size is not small enough to show a distinct variation of the band gap. It is clear from Fig. 5 that the PL emission does not show a blueshift corresponding to the blueshift in the transmission spectra in Fig. 1. Hence, the PL measurement demonstrates that the emission comes from the ZnO nanocrystals, and the blueshift in the transmission spectra (Fig. 1) is due to the amorphous phase in the film.

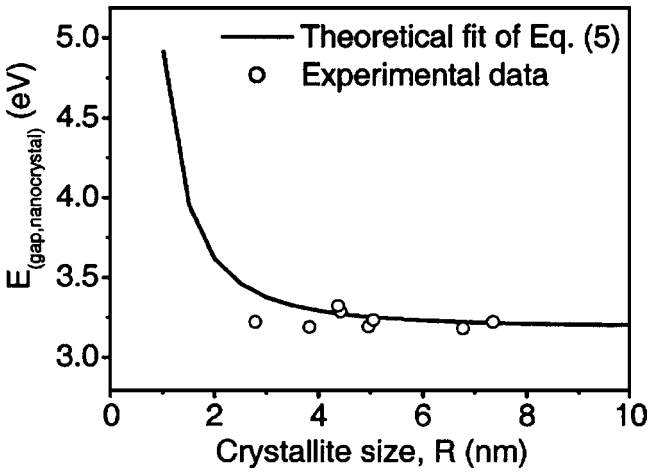

FIG. 5. Plot of $E_{(\mathrm{gap,nanocrystal})}$ obtained from PL measurement vs the nanocrystal radius R for ZnO films grown at various temperatures (○) and a theoretical fit using Eq. (5).

IV. CONCLUSIONS

In conclusion, the optical band-gap blueshift of ZnO thin films made of amorphous and nanocrystalline phases was studied. The amorphous phase in ZnO films obtained in films deposited at low temperature is believed to be the main reason for the blueshift of optical band gap. The estimated optical band gap of ZnO thin film blueshifts from 3.13 to 4.06 eV as the growth temperatures decreased from 500 to 200 °C. The estimated optical band gap shifts back to normal value after the annealing process. The PL emission does not blueshift as in the transmission spectra indicating the existence of nanocrystals embedded in the amorphous matrix of the ZnO films.

ACKNOWLEDGMENTS

The sponsorship from Agency for Science, Technology and Research (No. 0421010010), Singapore, is gratefully acknowledged. One of the authors (S.T.T.) was supported by a Postgraduate Scholarship from the Institute of Materials Research and Engineering, Singapore.

[1] M. H. Huang *et al.*, Science **292**, 1897 (2001).
[2] G. D. Mahan, J. Appl. Phys. **54**, 7 (1983).
[3] K. Keis, E. Magnusson, H. Lindstrom, S. E. Lindquist, and A. Hagfeldt, Sol. Energy Mater. Sol. Cells **73**, 51 (2002).
[4] D. Gruber, F. Kraus, and J. Muller, Sens. Actuators B **92**, 81 (2003).
[5] S. W. Kim, S. Fujita, and S. Fujita, Appl. Phys. Lett. **81**, 5036 (2002).
[6] X. W. Sun and H. S. Kwok, J. Appl. Phys. **86**, 408 (1999).
[7] R. F. Service, Science **276**, 895 (1997).
[8] X. W. Sun, S. F. Yu, C. X. Xu, C. Yuen, B. J. Chen, and S. Li, Jpn. J. Appl. Phys., Part 2 **42**, L1229 (2003).
[9] J. M. Bian, X. M. Li, X. D. Gao, W. D. Yu, and L. D. Chen, Appl. Phys. Lett. **84**, 4 (2004).
[10] A. V. Singh, R. M. Mehra, A. Wakahara, and A. Yoshida, J. Appl. Phys. **93**, 396 (2003).
[11] S. T. Tan, B. J. Chen, X. W. Sun, X. Hu, X. H. Zhang, and S. J. Chua, J. Cryst. Growth (to be published).
[12] H. C. Ong, J. Y. Dai, K. C. Hung, Y. C. Chan, R. P. H. Chang, and S. T. Ho, Appl. Phys. Lett. **77**, 1484 (2000).
[13] H. C. Ong, J. Y. Dai, A. S. K. Li, G. T. Du, R. P. H. Chang, and S. T. Ho, J. Appl. Phys. **90**, 1663 (2001).

[14]J. Tauc, *Amorphous and Liquid Semiconductors* (Plenum, London, 1974).
[15]E. A. David and N. F. Mott, Philos. Mag. **22**, 903 (1970).
[16]J. G. Lu, Z. Z. Ye, L. Wang, J. Y. Huang, and B. H. Zhao, Mater. Sci. Semicond. Process. **5**, 491 (2003).
[17]G. K. Williamson and W. H. Hall, Acta Metall. **1**, 22 (1953).
[18]Y. Kayanuma, Phys. Rev. B **38**, 9797 (1988).
[19]K. K. Kim, N. Koguchi, Y. W. Ok, T. Y. Seong, and S. J. Park, Appl. Phys. Lett. **84**, 3810 (2004).
[20]S. J. Pearton, D. P. Norton, K. Ip, Y. W. Heo, and T. Steiner, Prog. Mater. Sci. **50**, 293 (2005).
[21]G. Beni and T. M. Rice, Phys. Rev. B **18**, 768 (1978).
[22]W. J. Fan, J. B. Xia, S. T. Tan, and X. W. Sun (unpublished).